Santiago-Portillo, A.; Blandez, JF.; Navalón Oltra, S.; Alvaro Rodríguez, MM.; García Gómez, H. (2017). Influence of the organic linker substituent on the catalytic activity of MIL-101(Cr) for the oxidative coupling of benzylamines to imines. Catalysis Science & Technology. 7(6):1351-1362. doi:10.1039/c6cy02577c

Journal Name

ARTICLE

Influence of the organic linker substituent on the catalytic activity of MIL-101(Cr) for the oxidative coupling of benzylamines to imines

Received 00th January 20xx,
Accepted 00th January 20xx

DOI: 10.1039/x0xx00000x

www.rsc.org/

Andrea Santiago-Portillo,[a] Juan F. Blandez,[a] Sergio Navalón,[a] Mercedes Álvaro[a] and H. García[b,*]

MIL-101(Cr) having substituents at the terephthalate linker (X=H, NO_2, SO_3H, Cl, CH_3 and NH_2). promotes the aerobic oxidation of benzylamine to the corresponding N-benzylidene benzylamine at different rates. MIL-101(Cr)-NO_2 was the most active catalysts, about 6-fold more active than the parent MIL-101(Cr). MIL-101(Cr)-NO_2 does not deactivate significantly upon five consecutive reuses, does not leach metal to the solution and maintains its crystallinity. MIL-101(Cr)-NO_2 is active for a wide range of benzylamines including para-substituted, heterocyclic benzylamines and di- and tribenzylamines.

1. Introduction

Metal organic frameworks (MOF) have become among the favorite solid catalysts for liquid phase reactions,[1-8] because they combine large surface area, high transition metal content and being crystalline materials, they can be well characterized by XRD and porosimetry. [6, 9-11] One of the most widely used MOFs in catalysis is MIL-101 in where trimeric octahedra having a central M^{3+} ion (M^{3+}: Cr^{3+} or Fe^{3+}) share a common µ3O atom. Each trimeric M3µO nodal unit is coordinated to six terephthalate linkers. Four trimeric metal nodes and six connecting terephthalate linkers define a supertetrahedra block that by connecting with other twelve terephthalates (three per each metal node) define a tridimensional structure having two types of cages with hexagonal (8.6 Å) and pentagonal (5.5 Å) windows and dimensions of 1.6 and 1.2 nm in diameter, respectively. [10, 12-14] Each metal ion has an additional exchangeable coordination position, not compromised with the structure of the material that in two of three metal ions of the trimeric unit is typically occupied by water, dimethylformamide (DMF) depending on the synthesis condition and pretreatments. [14, 15] Upon adequate activation, the ligand occupying the exchangeable position can be removed, creating a coordination site that is able to interact with substrates or reagents.[16, 17]

Besides the presence of catalytic sites in activated MIL-101 materials by evacuation of the solid in the pretreatment process, one of the main features of MIL-101 is its remarkable structural stability and robustness under a wide range of conditions that make this crystalline solid compatible with the conditions required in a large number of liquid phase reactions. [16-21]

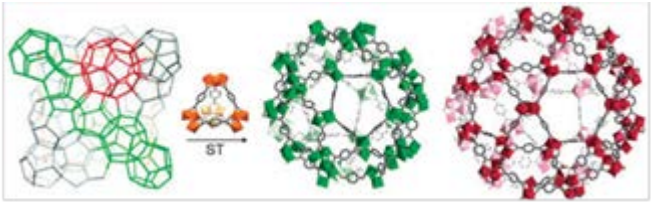

Figure 1. Schematic 3D representation of MIL-101 made of smaller (green) and larger (red) cages connected through super tetrahedra (ST). The illustration shows in the left the ensemble of the two types of cages and in the right isolated cages of each type of cavity. Reprinted with permission from ref.[15]

One reaction type that is currently under the spotlight using MOFs as solid catalysts is aerobic oxidations. [22, 23] The interest in this type of oxidation derives from the clear advantages of using molecular oxygen as oxidant, the well-known activity of transitions metals to promote this reaction class and the possibility to control the product distribution by performing the reaction in a confined space defined by the MOF pores. [3, 17, 21, 24, 25] In this context, some years ago the catalytic activity as radical initiator of N-hydroxyphthalimide (NHPI) adsorbed within commercial Basolite F300 (Fe as metal, 1,3,5-benzenetricarboxylate, BTC, as organic linker) to promote the aerobic oxidation of benzylamines into their corresponding N-benzylidene benzylamines through oxidative coupling (Eq. 1) was reported. [26] Although the use of Basolite F300 is

[a] *A. Santiago-Portillo, J. F. Blandez, Dr S. Navalón, Prof. M. Álvaro.*
Departamento de Química
Universidad Politécnica de Valencia
C/Camino de Vera, s/n, 46022, Valencia, Spainress here.
[b] *Prof. H. García,*
Departamento de Química and Instituto de Tecnología Química CSIC-UPV
Universidad Politécnica de Valencia
C/Camino de Vera, s/n, 46022, Valencia, Spain
E-mail: hgarcia@qim.upv.es
† Supporting information for this article is given via a link at the end of the document.

advantageous due to its commercial availability, one of the major drawbacks of the reported process is that Basolite F300 has so far, an unknown structure, making difficult to rationalize the reaction mechanism and to develop more efficient catalysts based on the kinetic data obtained from this material. [27]

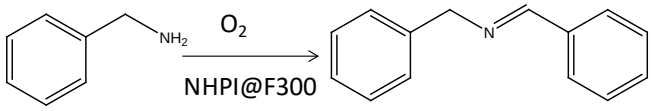

Equation 1. Oxidation of benzylamine to N-benzylidene benzylamine using NHPI@F300 as catalyst.[25]

Continuing with this line of research it is of interest to study the oxidative coupling of benzylamines in the presence of other MOFs with a well-defined crystalline structure. In this context, an important feature of MOFs that make these materials so promising to promote reactions as liquid phase is the versatility in their synthesis that allows a considerable degree of tunability in their properties including catalytic activity. [2-5, 28-33] In this way, a strategy that could increase the activity of a family of MOFs[28] and, specifically, the activity of MIL-101(Cr) would be the use of substituted terephthalic acids as components, resulting in the formation of isostructural MIL-101(Cr) solids. [34] By using substituted terephthalates, the electron withdrawing or donating effect of the substituent on the aromatic dicarboxylic linker would influence the electronic density around the nodal metal ions acting as active sites, thus, allowing a degree of control on the strength of these actives sites as Lewis acids and as redox centers. [28] In this context, the synthesis of MIL-101(Cr) with a series of substituted terephthalates has been already reported in the literature, [35-43] although as far as we know they have not yet been used in catalysis as a way to optimize and enhance the catalytic activity of these materials.

In the present work we have prepared a series of five MIL-101(Cr)-X (X= H, Cl, SO_3, NO_2, CH_3) materials and evaluated their activity as promoters of the aerobic oxidation of benzylamines to N-benzylidene benzylamine (Eq. 1). In a pioneer precedent, Speybroeck, de Vos and coworkers have shown that substitution in terephthalic acid has a strong influence on the catalytic activity of UiO-66 as Lewis acids. [28] Following this work, we have expanded this type of studies to a different MOF, MIL-101 and also to a different reaction type, aerobic oxidation in the present case. Activity data of substituted MOFs can eventually lead to their optimization as promoters of oxidations. This methodology illustrates the advantages that MOFs offer with respect to other types of porous solids where organic chemistry concepts on the influence of substitution cannot be applied.

2. Results and Discussion

2.1. Catalyst characterization

The synthesis of the series of MIL-101(Cr)-X was carried out by reaction of a Cr^{3+} salt (nitrate or chloride) and the corresponding substituted terephthalic acid in demineralized water at an adequate temperature (180-200 ºC), following reported procedures (Scheme 1). [10, 34] In the cases of MIL-101(Cr)-SO_3H and MIL-101(Cr)-NH_2 the materials were obtained from pre-formed MIL-101(Cr)-H and MIL-101(Cr)-NO_2, respectively, by sulfonation[44] and chemical reduction, [45] as reported in the literature (Scheme 1).

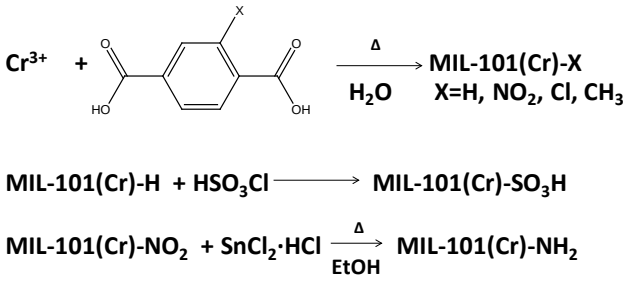

Scheme 1. Synthesis of MIL-101(Cr)-X (X= H, NO_2, Cl, CH_3, SO_3H, and NH_2).

Powder X-ray diffraction (XRD) of the series of five substituted MIL-101(Cr)-X show that all the materials are isostructural with the pattern MIL-101(Cr)-H with coincident unit cell parameters, as already reported in the literature. [34, 44, 45] Figure 2 shows the XRD patterns of the materials under study. BET surface area and pore volume of the series of MIL-101(Cr)-H were measured by isothermal N_2 adsorption with values from 2735-1,240 $m^2 \times g^{-1}$ and 2.16-1.02 $cm^3 \times g^{-1}$, respectively, that are in the range of those that have been reported in the literature. [17, 34] Supporting information (Figures S1-S6) shows the corresponding isothermal adsorption plots from which the BET and pore volume values had been determinated. Table 2 lists the BET surface area values for each of the materials under study. As it was reported, the presence of substituents in the aromatic ring decreases somewhat the surface area and pore volume with respect to the unsubstituted parent MIL-101(Cr)-H due to the space needed to accommodate the organic substituent. [34] The presence of substituent on the terephthalate organic linker can be determined by FT-IR spectroscopy. [34] Figure 3 presents the FT-IR spectra of the MIL-101(Cr)-X used in this study, while Table 2 lists also the most characteristic vibration bands due to the presence of the corresponding substituent. Figures S7-S12 show the FT-IR spectra for each MIL-101(Cr)-X. The thermogravimetric profiles of the set of MIL-101(Cr)-X were also determined to establish their thermal stability, presence of co-adsorbed water and the percentage of organic linkers. Figures S13-S18 in the supporting information present the TG

plots for each sample, while the most relevant data are included in Table 1. In the case of MIL-101(Cr)-SO_3H, the S content was determined by combustion chemical analysis giving a value of 24, 5, 1% for the percentage of C, H and S, respectively. This sulphur content is similar to the one that has been reported in the literature for this material. [44] Overall, all the characterization data indicate that we have successfully prepared crystalline isostructural MIL-101(Cr)-X materials with coincident characterization data as previously reported offering us the possibility to evaluate their catalytic activity. [34, 44, 45]

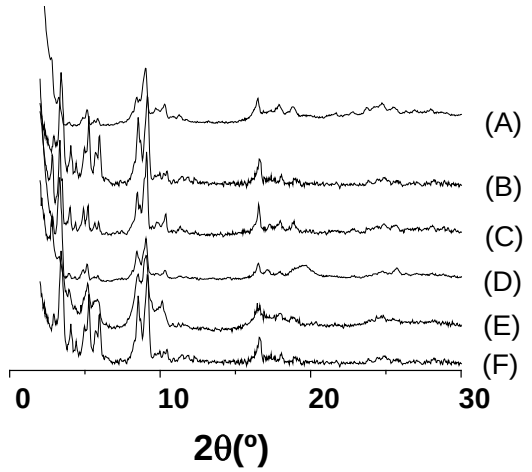

Figure 2. XRD patterns of MIL-101(Cr)-H (A), MIL-101(Cr)-NO_2 (B), MIL-101(Cr)-SO_3H (C), MIL-101(Cr)-Cl (D), MIL-101(Cr)-CH_3 (E), MIL-101(Cr)-NH_2 (F).

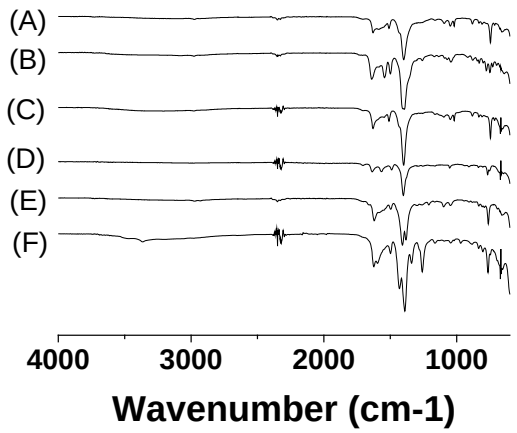

Figure 3. IR of MIL-101(Cr)-H (A), MIL-101(Cr)-NO_2 (B), MIL-101(Cr)-SO_3H (C), MIL-101(Cr)-Cl (D), MIL-101(Cr)-CH_3 (E), MIL-101(Cr)-NH_2 (F).

Table 1. List of catalyst employed in the present study with their corresponding textural, stability and most relevant IR spectroscopic bands.

Catalysts	BET Surface area ($m^2 \times g^{-1}$)	Pore volume ($cm^3 \times g^{-1}$)	Theoretical metal content (%) / Calculated from TG	IR bands, υ (cm^{-1})
MIL-101(Cr)-H	2,740	2.2	21.77/22.84	3200 (OH), 3050 (C-H aromatic), 1640 (carboxylate) and 1515 (C=C aromatic)
MIL-101(Cr)-NO_2	1,800	1.3	17.56/18.28	1500 and 1380 (NO_2)
MIL-101(Cr)-SO_3H	1,550	1.3	20.76/21.68	1160 (SO_3H)
MIL-101(Cr)-Cl	1,250	1.1	17.47/24.8	760 (C-Cl)
MIL-101(Cr)-CH_3	1,780	1.8	21.04/18.62	2980-2850 (CH_3) and 1360 (CH_3)
MIL-101(Cr)-NH_2	1,930	2.0	20.97/22.90	3450 (NH_2) and 1630 (NH_2)

2.2 Catalytic activity

With the set of MIL-101(Cr)-X samples prepared, we carried out the aerobic oxidation of benzylamine to the corresponding oxidative coupling product. This reaction has been one of the favourite benchmark tests to evaluate the catalytic activity of a series of solid catalysts including supported noble metal nanoparticles such as gold. [26, 46-48] More closely related to the present work, we have reported that adsorption of NHPI on commercially available FeBTC is a suitable catalyst to promote this oxidation. [26] In the present study, benzylamine oxidation was observed in the presence of the series of MIL-101(Cr)-X as catalysts. Importantly, the initial reaction rate and conversion at final reaction times were strongly dependent on the substitution on the terephthalate linker. Figure 4 shows the temporal profiles of benzylamine conversion in the presence of each of the MIL-101(Cr)-X catalyst. A control experiment under the same conditions in the absence of catalyst shows no benzylamine conversion in the present reaction conditions. In all cases N-benzylidene benzylamine was the only reaction product observed with selectivity over the time higher than 95 %. Table 2 compiles the initial reaction rates (r0) and benzylamine conversion at final reaction time.

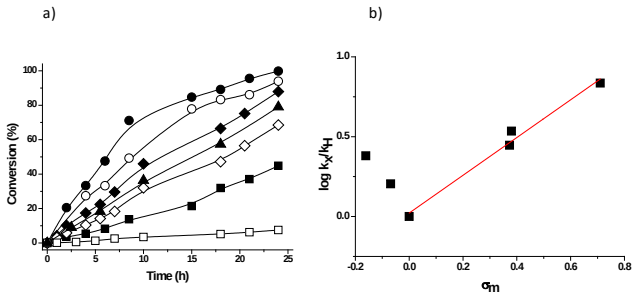

Figure 4. a) Time-conversion plot for the aerobic oxidation of benzylamine to N-benzylidene benzylamine using each MIL-101(Cr)-X as catalyst. Legend: MIL-101(Cr)-H (■), MIL-101(Cr)-NO_2 (●), MIL-101(Cr)-SO_3H (○), MIL-101(Cr)-Cl (♦), MIL-101(Cr)-CH_3 (◊), MIL-101(Cr)-NH_2 (▲) and blank control in the absence of catalyst (□). Reaction conditions: Catalyst (0.04 mmol of Cr), substrate (20 mmol), 120 ºC, O_2 atmosphere. b) Hammett plot.

Table 2. Initial reaction rates, final conversions and oxidation potentials for the series of MOFs under study. Reaction conditions: Catalyst (0.04 mmol of Cr), substrate (20 mmol), 120 ºC, O_2 atmosphere.

Catalysts	r_0 (mM h^{-1})[a]	Conv. at 24 h (%)	$E_{1/2}$ (V)[B]
MIL-101(Cr)	1.82	45	0.4025
MIL-101(Cr)-NO_2	12.5	>95	0.5135
MIL-101(Cr)-SO_3H	6.25	94	0.4525
MIL-101(Cr)-Cl	5.1	88	0.4065
MIL-101(Cr)-CH_3	2.5	68.5	--
MIL-101(Cr)-NH_2	3.8	78	--

[a] Determined form the time conversion plot by measuring the slope of the conversion plot at zero time. [b] Determined as the semi sum of the peak potential of the forward and backward scan.

In an attempt to rationalize the influence of the nature of the substituent, a plot of the logarithm of the relative initial reaction rate of MIL-101(Cr)-X respect MIL-101(Cr)-H versus the Hammett σ parameter of each substituent was made. Of the various Hammett parameters possible, the one that fits better with the experimental values for a linear relationship was the one corresponding to the meta position, σ_m. It should be noted that each terephthalate is connected simultaneously to two metal nodes and for one of them the substituent is in meta position and for the other is in the para position. Therefore, the use of any of the two σ_m and σ_p constants could be reasonable. The results are presented also in Figure 4. As it can be seen there, a reasonable straight line for the log kX/kH vs σ_m was obtained for four catalysts, but not for the cases of electron donating substituents MIL-101(Cr)-NH_2 and MIL-101(Cr)-CH_3, respectively. It could be that besides influencing the electron density on the metal nodes these two substituents could have a different role promoting or stabilizing the reaction intermediates. The ability of $-NH_2$ to form hydrogen bonds and donate electrons, and the possibility to form benzyl radicals with the $-CH_3$ substituents, may play a role different than just inductive effects. MIL-101(Cr)-NH_2 and MIL-101(Cr)-CH_3 exhibit about 4 and 2 times higher initial reaction rate than expected according to its σ_m constants, respectively. According with the trend observed in Figure 4, it seems that the presence of electron withdrawing substituents increases the catalytic activity around the Cr^{3+} node, due to the operation of inductive effects that should decrease the electron density around the Cr^{3+} ions.[28, 49] Experimental evidence for the influence of substitution at the terephthalate on the Cr^{3+} ion was obtained by cyclic voltammetry. Figure 5 shows the cyclic voltammetry of MIL-101(Cr)-H compared to MIL-101(Cr)-NO_2 and supporting information provides the full set of cyclic voltammetries for the other samples (Figures S19-S22). As it can be seen in Figure 5 MIL-101(Cr)-H exhibits under the conditions used an oxidation peak at 0.503 V, appearing at lower oxidation potential than in the case of MIL-101(Cr)-NO_2. In this case, a quasi-reversible oxidation peak was determined at 0.577 V. We attribute this shift in the oxidation peak of Cr^{3+} ions to the influence of the electron withdrawing nitro groups that will made Cr^{3+} oxidation more difficult. In support of this rationalization the MIL-101(Cr)-Cl and MIL-101(Cr)-SO_3H show also higher potential for the oxidation of Cr^{3+} ions than the parent MIL-101(Cr)-H depending on the substituent. These values of $E_{1/2}$ measured for MIL-101(Cr)-X are also collected in Table 2.

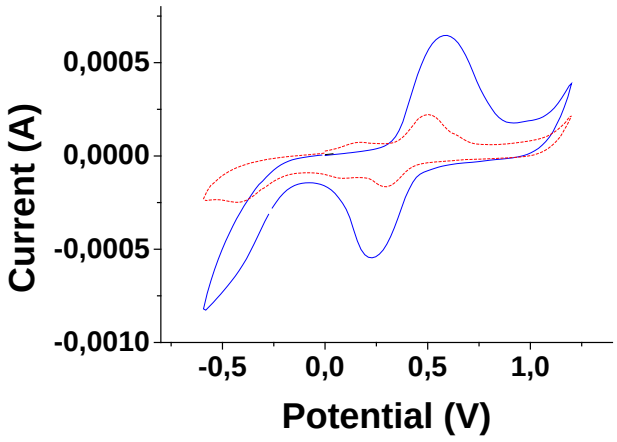

Figure 5. Cyclic voltammograms (scan rate 50 mV/s) in the range +1.2 V > E > -0.6 V of MIL-101(Cr) immobilized at the surface of a pyrolytic graphite electrode and using aqueous acetic acid 0.1M as electrolyte. MIL-101(Cr)-NO_2 (continuous blue line) and MIL-101(Cr)-H (dotted red line).

Based on the experimental data obtained by cyclic voltammetry on the ease of Cr^{3+} oxidation in MIL-101(Cr)-X depending on the substituent, we propose that the higher catalytic activity observed by MIL-101(Cr)-NO_2 derives from its ability to promote the initial oxidation of benzylamine by electron transfer from electron rich amine as donor to the Cr_3-μO cluster

as electron acceptor, initiating an autooxidation mechanism involving benzylic radicals. Scheme 2 summarizes our mechanism proposal.

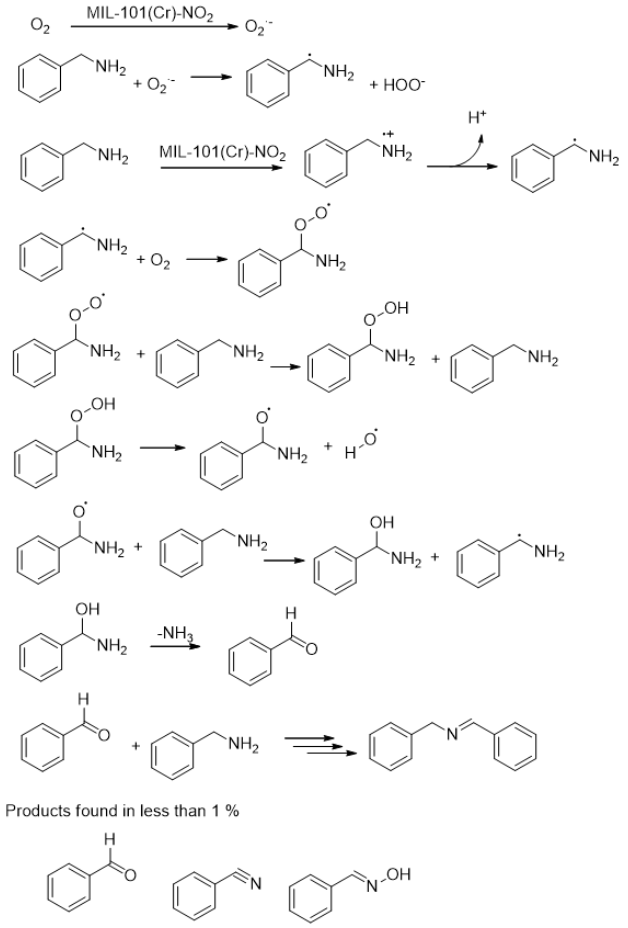

Scheme 2. Mechanism proposal for the aerobic oxidation of benzylamine by MIL-101(Cr)-NO_2.

In support of the occurrence of a radical chain autooxidation mechanism, we performed a hot filtration test to determine the influence of the removal of the solid catalyst once the reaction has been initiated. Figure 6 shows the time conversion plots for two twin reactions, one that was in contact with the MIL-101(Cr)-NO_2 during the complete reaction time and the other in which the solid catalyst was removed by filtration at the reaction temperature (120 ºC) at 6 h when the conversion was about 48 %. As it can be seen in Figure 6, there is almost no influence of the presence or absence of catalyst once the reaction has been initiated and reaches a conversion about one half of the final value. There could be two alternative explanations to understand the reasons why the reaction of the hot filtration test progresses in the absence of solid similarly to the twin reaction in the presence of catalyst. The simplest one would be leaching of chromium as active site from the solid to the solution and occurrence of the reaction in homogeneous phase. In radical chain autooxidations it is known that just small amounts of metals, even in the ppb region, can be active to initiate these reactions.[50] However, control experiments using chromium acetate in the amount as well as twice the amount determined by ICP in solution for the leached Cr shows that with these minute amounts the progress of the reaction is considerably slower and only a conversion of 10 % at final reaction time (Figure 6) can be achieved.

A second alternative possibility to explain the progress of the reaction after filtration of the solid would be that MIL-101(Cr)-NO_2 is acting as radical initiator of benzylamine autooxidation. In this second explanation, the role of MIL-101(Cr)-X is more like a radical initiator than a true catalyst for this aerobic oxidation. It should be, however, commented that as it can be seen in Figure 4, a blank control in the absence of any catalyst under the reaction conditions at 120 ºC does not result in any significant benzylamine conversion for 23 h.

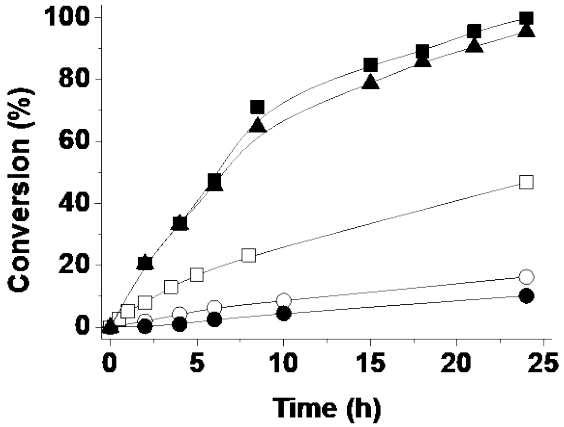

Figure 6. Time-conversion plot for the aerobic oxidation of benzylamine to N-benzylidene benzylamine using MIL-101(Cr)-NO_2 as catalyst that is filtered at 4 h reaction time or that remains in contact with the substrate for the full reaction time. Controls experiments with $Cr(OAc)_3$ as homogeneous catalysts are also shown. Legend: MIL-101(Cr)-NO_2 (■) and after catalyst filtration at 4 hours (▲), Chromium acetate with the amount of Cr present in the MOF (□), Chromium acetate with the amount of leached Cr found in the reaction (●) and chromium acetate with twice the amount of leached Cr (○). Reaction conditions: Catalyst (12 mg MIL-101(Cr)-NO_2 equivalent to 0.04 mmol of Cr), substrate (20 mmol), 120 ºC, O_2 atmosphere.

After having shown the activity of MIL-101(Cr)-X for benzylamine oxidation, it was of interest to gain information about the reaction mechanism and, particularly, how benzylamine or oxygen is activated by MIL-101(Cr) catalyst. Thus, we performed and electron paramagnetic resonance spectroscopy (EPR) study of molecular O_2 activation by MIL-101(Cr)-H compared to MIL-101(Cr)-NO_2. The experiments were carried out using PBN as spin trapping agent, in dodecane as solvent in the absence of benzylamine, trying to characterize spectroscopically the PBN adduct of any possible reactive oxygen species that could be generated by the MOFs. The results are presented in Figure 7 and experimental section describes in detail the conditions of the experiments. As it can be seen there, just heating in the absence of any MOF catalyst

allows the detection of the adduct between hydroperoxyl radical (HOO·) and PBN. Under the same conditions the presence of MIL-101(Cr)-H increases significantly the concentration of this adduct, being, however, the signal of the PBN-OOH adduct was even much more intense (about one order of magnitude higher than in the case MIL-101(Cr)-H and two orders of magnitude higher than the blank control) when MIL-101(Cr)-NO_2 was used as initiator. Figure 7 also presents the simulated EPR spectra for the PBN-OOH adduct showing that, although there is not a strict coincidence on the expected relative intensity of some of the PBN-OOH signals, [21] the position and hyperfine coupling of the experimental EPR spectrum exactly coincide with those of the simulated spectrum for PBN-OOH, thus providing a strong support for the generation of HOO· radicals, particularly in the presence of MIL-101(Cr)-NO_2. It is important to note that some authors have reported degradation of the PBN under the reaction conditions required for spin trap and, therefore, recording some variations respect to the exact spectrum of the expected PBN-OOH adduct could be possible. [51, 52] Although the conditions of the EPR measurements do not guarantee a rigorous quantification of the amount of HOO radicals generated, they gave a clear qualitative indication that the most efficient material for oxygen activation is MIL-101(Cr)-NO_2, showing in this way the influence of the substitution of the terephthalate linker on the material. Scheme 2 shows the set of reactions that according to the literature are the most probable processes resulting in oxygen activation. [17, 21, 26]

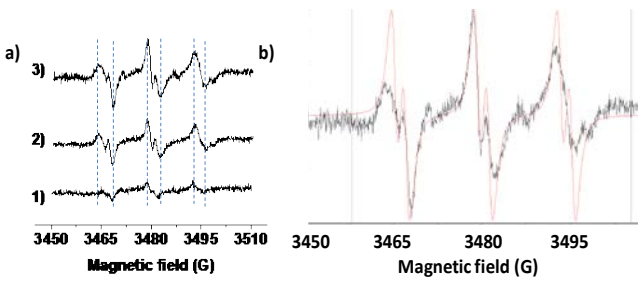

Figure 7. a) Experimental EPR spectra using (1) PBN + O_2, (2) MIL-101(Cr)-H + PBN + O^2 and (3) MIL-101(Cr)-NO_2 + PBN + O_2. The experiments were carried out using n-dodecane as solvent at 120 ºC for 4 h. b) Experimental and simulated EPR spectra of PBN-OOH adduct under (3) conditions. Experimental hyperfine coupling constants of PBN-OOH coinciding with those reported in literature AGN = 14.0 and AGH = 2.05.

In further support of these equations resulting in formation of hydroperoxyl radicals, the presence of H_2O_2, the most likely final product of O_2 reduction derived from ·OOH, was also detected by standard colorimetric conditions (see experimental section and supporting information Figure S.23) in much higher concentration for MIL-101(Cr)-NO_2 than for MIL-101(Cr)-H reaching a maximum concentration of 110 ppm (3.25 mM H_2O_2).

Scheme 2 shows several different reactive oxygen species (ROS) that could be responsible for attack at the benzylic position of benzylamine, initiating the oxidative coupling that eventually will lead to the final N-benzylidene benzylamine. It is possible that all of these ROS contribute in various degrees to the generation of the benzylamine radical or it could be that benzylamine oxidation is predominantly due to just a single ROS species. To address this issue and to gain additional information on the oxidation mechanism, a series of three quenching experiments were performed. In these experiments the aerobic oxidation of benzylamine in the presence of MIL-101(Cr)-NO_2 was carried out adding dimethylsulfoxide (DMSO), p-benzoquinone or 2,2,6,6-tetramethyl-1-piperidinyloxy (TEMPO). There are abundant literature data showing that DMSO selectively quenches hydroxyl radicals resulting in the formation of methanesulfinic acid. [17, 21, 53, 54] In contrast, p-benzoquinone is a selective quencher of superoxide ($O^{2\cdot-}$).[17, 21, 55] while TEMPO reacts with carbon-centred benzylic radicals. [17] The lack of $^1O_2$ as intermediate under non-irradiated conditions was convincingly proved by the lack of NaN_3 quenching (data not shown). NaN_3 is a selective $^1O_2$ quencher.[56] The results of these quenching studies are shown in Figure 8 that plots the temporal profiles of a series of four reactions, in three of them the quencher was added at 5 h of reaction time, while no quenchers were added in the fourth experiment. It should be noted that none of the quenchers was able to stop completely the reaction, a fact that can be understood considering that activation of oxygen by MIL-101(Cr) takes place continuously, regardless the presence of quencher, inside the cavities of the material and, due to diffusion restrictions, complete quenching cannot be expected under continuous ROS generation. However, as it can be seen in this Figure, the presence of p-benzoquinone or TEMPO decreases considerably conversion of benzylamine, indicating that, as expected, superoxide and carbon center radicals are the most important intermediates involved in the oxidation.

More surprising was the influence of DMSO, since this quencher is specific for HO· radicals and it is unable to quench hydroxyperoxyl radicals (HOO·).[17, 53] As it can be seen in Figure 8 the presence of DMSO decreases the reaction of benzylamine, although in about one half compared to the effect of p-benzoquinone. Accordingly, it seems that, somehow, in the building up of ROS and the generation of H_2O_2, MIL-101(Cr)-NO_2 is able to generate also HO radicals that would contribute partly to the total benzylamine oxidation. After generation of benzylamine radical the subsequent steps will involve, as proposed in the literature, [26] formation of benzylimine intermediate, followed by nucleophilic attack of benzylamine to benzylimine and final deamination (see Scheme 2).

Having determined that the role of MIL-101(Cr)-X in the aerobic oxidation of benzylamine is more as promoter, activating molecular O_2, than a real catalyst with turnover cycles, each cycle involving the participation of the active site in the MOF, we proceeded to optimize the amount of catalyst. Figure 9 shows the temporal profile of benzylamine conversion

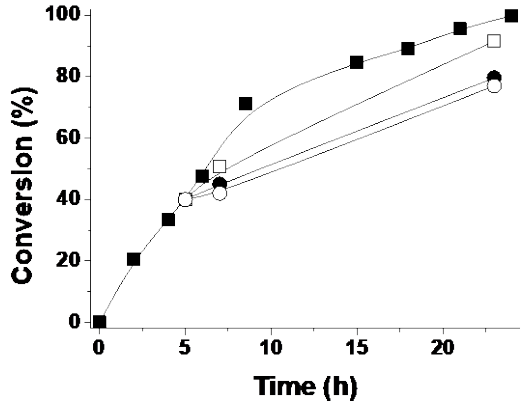

Figure 8. Time-conversion plot for the aerobic oxidation of benzylamine to N-benzylidene benzylamine using MIL-101-NO_2(Cr) as catalyst. Legend: MIL-101-NO_2(Cr) (■), 20% DMSO (□), 20% p-benzoquinone (●) and 20% TEMPO (○). Reaction conditions: 12 mg MIL-101(Cr)-NO_2 (0.04 mmol of Cr), 20 mmol substrate, 120 ºC, O_2 atmosphere.

as a function of the amount of MIL-101(Cr)-NO_2. It was observed that increasing the amount of catalyst increases the reaction rate, but, there were like to different regimes, the initial one occurring for low amounts of MIL-101(Cr)-NO_2 characterized by a larger slope in the plot of initial reaction rate vs weight of catalyst present and a second regime with smaller slope. The amount of catalyst in which the regime changes is about 6 mg under our experimental conditions. This indicates that smaller amounts of catalyst are, in comparison, more efficient in promoting the reaction and further increase for weights of catalyst larger than 6 mg the growth of the reaction rate became less important. The two regimes could be caused by the constant O_2 concentration in the liquid phase and a more efficient generation of hydroperoxyl radicals and ROS for low weights of catalysts. For higher catalyst amounts, the limiting factor would be the concentration of dissolved oxygen, rendering the process per active site less efficient.

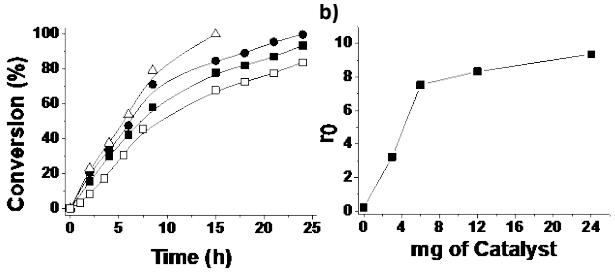

Figure 9. a) Time-conversion plot for the aerobic oxidation of benzylamine to N-benzylidene benzylamine using different amounts of MIL-101(Cr)-NO_2 as catalyst. Legend: 3 mg of MIL-101(Cr)-NO_2 (□), 6mg of MIL-101(Cr)-NO_2 (■), 12 mg of MIL-101(Cr)-NO_2 (●), 24 mg of MIL-101(Cr)-NO_2 (Δ). b) Initial rate-mg of Catalyst plot.

To check this proposal we performed three additional experiments in where the atmosphere was argon, air and oxygen, respectably. The results are presented in Figure 9. As it can be seen there, under argon benzylamine conversion was very low (less than 10 %) at 24 h reaction time, in agreement with the requirement of an oxidant to achieve stoichiometric oxidation. The low conversion measured could be due to MOF acting as reagent rather than as a catalyst. If after 24 h under argon the atmosphere is changed to oxygen, then the reaction proceeds with a similar profile as that measured when the reaction is initiated under oxygen. When the reaction is performed under air, due to the lower oxygen pressure under these conditions compared to pure oxygen, a decrease in the initial reaction rate and final conversion at 24 h were observed. This behavior agrees with solubility of oxygen in the liquid phase as being the limiting factor in benzylamine oxidation. Moreover a linear relationship between initial reaction rate and partial O_2 pressure was obtained, indicating that the reaction is first order with respect to oxygen pressure (see Figure 10b).

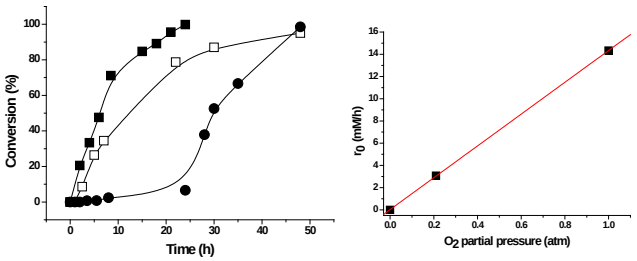

Figure 10. a) Influence of the reaction atmosphere on the time-conversion plot during the benzylamine reaction in the presence of MIL-101(Cr)-NO_2. Legend: O_2 (■), air (□), Ar for 24 h and then O_2 (●). Reaction conditions: 12 mg MIL-101(Cr)-NO_2 (0.04 mmol of Cr), 20 mmol substrate, 120 ºC. b) Partial pressure plot of benzylamine oxidation.

The catalytic stability of MIL-101(Cr)-NO_2, that is the most active material for benzylamine aerobic oxidation, was confirmed by performing consecutive uses of the same sample and following the temporal evolution of benzylamine conversion in each reaction. After each run, MIL-101(Cr)-NO_2 was recovered from the reaction by filtration, washed with ethanol and dried at 60 ºC before the next reuse. The results of the reuse experiments are presented in Figure 11. As it can be seen there, MIL-101(Cr)-NO_2 maintains quite constant the initial reaction rate upon reuse, reaching at final reaction time essentially complete conversion. This supports the stability of the sample under the reaction conditions. Moreover, crystallinity of the several times used material was checked by performing XRD of the sample (see insert of Figure 11). As it can be seen there, no change in the XRD was observed, indicating that the structure is well maintained during the reaction. In addition, chemical analysis of the liquid phase after removal of the catalyst showed that the amount of Cr present in the solution was 0.5 % of the total Cr amount present in the fresh catalyst. This stability agrees with previous reports using MIL-101(Cr)-H as catalyst for aerobic oxidations in liquid phase that have shown that this particular MOF is considerably robust under typical reaction conditions. [17-21]

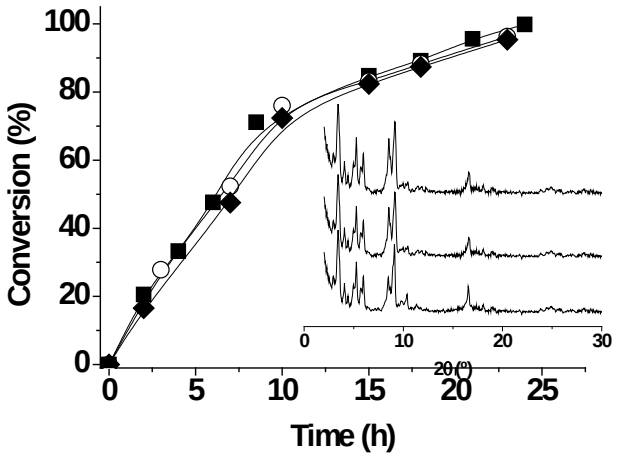

Figure 11. Reusability experiments of MIL-101(Cr)-NO_2 as catalyst in the aerobic oxidation benzylamine to N-benzylidene benzylamine. Reaction conditions: Catalyst (12 mg), susbtrate (20 mmol), 120 ºC, O2 atmosphere. Legend: 1st use (■), 3th use (○), 5th use (♦). The temporal profiles of runs 2nd and 4th are also coincident and have not been plotted for the sake of clarity. Inset: XRD of fresh MIL-101(Cr)-NO_2 (A), three times used MIL-101(Cr)-NO_2 (B) and five times used MIL-101(Cr)-NO_2 (C).

An alternative experiment to show catalyst stability and performance is the so-called "productivity test" in which the reaction of benzylamine is carried out at much lower catalyst to substrate molar ratio. In the present case, we have performed an additional experiment using 200 mmol of benzylamine (21.4 g) and 0.02 % Cr to benzylamine molar ratio and followed the temporal evolution of benzylamine conversion until complete conversion. Figure 12 presents the time conversion plot of this

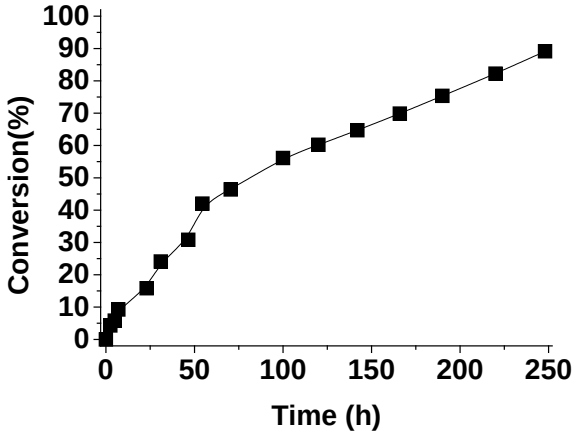

Figure 12. Time-conversion plot for the aerobic oxidation of benzylamine to N-benzylidene benzylamine under productivity test conditions using low MIL-101(Cr)-NO_2 to substrate ratio (■). Reaction conditions: Catalyst (10 mg, 0.033 mmol of Cr), substrate (21,4 g, 200 mmol) substrate, 120 ºC, O_2 atmospheric pressure.

productivity test showing that even using very small amount of catalyst in comparison to the amount of substrate the reaction progresses reaching complete conversion at sufficiently long reaction times, indicating that the catalyst does not undergo deactivation.

Activation energy for benzylamine oxidation using MIL-101(Cr)-NO_2 was determined by studying the influence of the reaction temperature on the initial reaction rate in the range from 120 to 140 ºC and using the Arrhenius plot. Figure 13 shows the temporal evolution of benzylamine conversion as a function of the reaction temperature and the corresponding Arrhenius plot. A fairly linear correlation between ln r_0 and 1/T (K^{-1}) was obtained allowing estimating from the slope of the linear plot an activation energy of 46 kJ×mol^{-1} for the process.

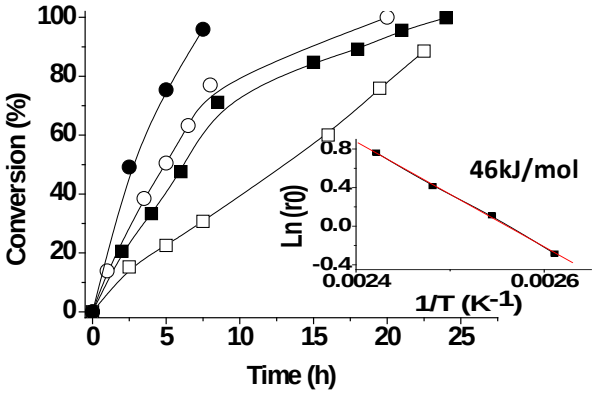

Figure 13. Time-conversion plot for the aerobic oxidation of benzylamine to N-benzylidene benzylamine using MIL-101(Cr)-NO_2 as catalyst carried out at four different temperatures. The inset shows the Arrhenius plot in the aerobic oxidation of benzylamine to N-benzylidene benzylamine based on the initial reaction rates r0 obtained from the time-conversion plot. Legend: 110 ºC (□), 120 ºC (■), 130 ºC (○), 140 ºC (●). Reaction conditions: Catalyst (12 mg, 0.04 mmol of Cr), substrate (20 mmol), O_2 atmosphere.

To show that substitution at the terephthalate linker influences the aerobic oxidation of benzylamines in general and that the relative order of solid activity is not determined by the substrate, we also performed the aerobic oxidation of 4 chlorobenzylamine using the series of five MIL-101(Cr)-X. It was observed that 4 chlorobenzylamine reacts in general faster than benzylamine, due to the electron withdrawing influence of the Cl atom on the substrate. Also for 4-chlorobenzylamine the series of MIL-101(Cr)-X exhibit different catalytic activity, following the same relative order as that previously indicated for the parent benzylamine. Moreover, the plot of the ln r_0 vs the Hammett σ_m constant for 4-chlorobenzylamine follows the same trend that was already presented for the parent benzylamine. Similarly as for benzylamine, the methyl substituted MIL-101(Cr)-CH_3 was five times more reactive than expected according to the σ_m Hammett parameter. This behavior with 4 chlorobenzylamine shows that the influence of substitution on the terephthalate on the catalytic activity of the

MIL-101(Cr) is a general effect, although it should be noted that the increase in the relative reaction rate of the NO_2 versus H is about 2.5 times lower for 4-chlorobenzylamine as substrate compared to the pattern benzylamine. Thus, the nature of the substrate also plays a role on the reaction rates and on the quantitative values of the promotional effect of the substitution on the terephthalic linker. This influence of substrate is also reflected on the different activation energy determined from the Arrhenius plot (see Figure 15) for 4-chlorobenzylamine (Ea 28.62 kJ/mol) compared to the pattern benzylamine (Ea 46 kJ/mol).

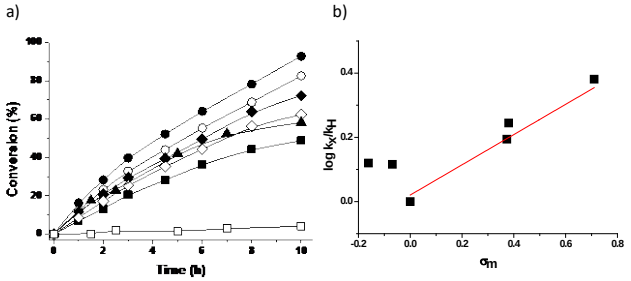

Figure 14. a) Time-conversion plot for the aerobic oxidation of 4-chlorobenzylamine to the corresponding N-benzylidene benzylamine using MIL-101(Cr) as catalyst. Legend: MIL-101(Cr) (■), MIL-101-NO_2 (Cr) (●), MIL-101-SO_3H (Cr) (○), MIL-101-Cl (Cr) (♦), MIL-101-CH_3 (Cr) (◊), MIL-101(Cr)-NH_2 (▲) and blank control (□). Reaction conditions: Catalyst (0.04 mmol of Cr), substrate (20 mmol), 120ºC, O_2 atmosphere. b) Plot of the relative initial reaction rate in logarithm scale versus the σ_m Hammett constant.

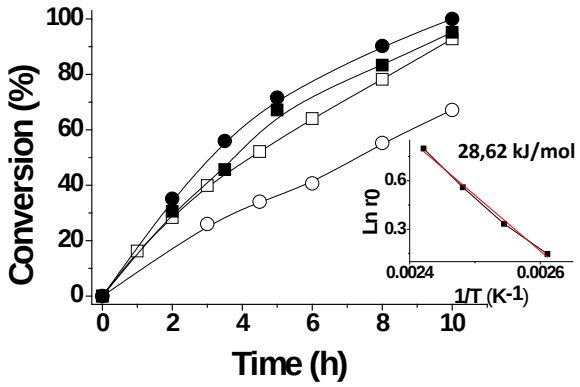

Figure 15. Time-conversion plot for the aerobic oxidation of 4-chlorobenzylamine to the corresponding N-benzylidene benzylamine using MIL-101(Cr)-NO_2 carried out at four different temperatures. The inset shows the Arrhenius plot for the aerobic oxidation of 4-chlorobenzylamine to the corresponding N-benzylidene benzylamine based on the initial reaction rates r0 obtained from the time-conversion plot. Legend: 110 ºC (○), 120 ºC (□), 130 ºC (■), 140 ºC (●). Reaction conditions: Catalyst (12 mg, 0.04 mmol of Cr), substrate (20 mmol), O_2 atmosphere.

The scope of benzylamine oxidation using MIL-101(Cr)-NO_2 as catalyst was checked by performing the reaction with three other substituents besides the parent benzylamine, two para-substituted benzylamines, namely 4-chloro and 4-methylbenzylamine, a heterocyclic benzylamine, 2-picolylamine, and a secondary dibenzylamine and a tertiary, tribenzylamine, substrates. The results are summarized in Table 3.

Table 3. Aerobic oxidation of benzylamine derivatives using MIL-101(Cr)-NO_2 as catalyst[a]

	Conversion (%)	Main reaction products	Selectivity (%)
4-Chlorobenzylamine	100	4-chlorobenzyl Idene 4chloro benzylamine	>99
4-Methylbenzylamine	100	4-methylbenzyl Idene 4-methyl benzylamine	>99
2-Picolylamine	85	Di-(2-picolyl)amine	67
Dibenzylamine	55	N-benzylidene benzylamine	>99
Tribenzylamine[b]	20	N-benzylidene benzylamine	75.8
		Dibenzylamine	24.2

[a] Reaction conditions: Catalyst (12 mg), substrate (20 mmol), O_2 atmospheric pressure, 120 ºC, 24 h for all substrates except for 4-chorobenzylamine (8 h). [b] Reaction temperature 140 ºC.

Although complete conversion of para-substituted benzylamines to the corresponding substituted N-benzylidenebenzylamine was achieved, it was observed that the presence of a substituent influences the reaction rate, 4-chlorobenzylamine reacting considerable faster than unsubstituted benzylamine and 4-methylbenzylamine the last being the substrate with lowest reaction rate. This influence of the substituent on the benzylamine substrate was quantitatively analyzed by plotting the initial reaction rate versus the σm Hammett constant of the substituent (see inset in Figure 16). From the linear relationship it can be concluded that the nature of the transition state has some anionic character, whereby electron withdrawing substituents such as Cl should increase the reaction rate by stabilizing the partial negative charge evolving at the benzylic position. In agreement with this proposal for the nature of the transition state, 2-picolylamine, having electron deficient pyridine heterocycle, also reacts quickly under the reaction conditions, although in these case 2-pycolylamide was the major product observed. In the case of dibenzylamine and tribenzylamine, formation of N benzylidene benzylamine was observed, as the only product in the case of dibenzylamine, or accompanied by the formation of some dibenzylamine in the case of tribenzylamine. The most salient feature for di- and tribenzylamines was, however, that the reaction rate was considerably slower than in the case of benzylamine, decreasing the reaction rate as the size of the substrate increases. In fact, in the case of tribenzylamine the reaction at 120 ºC was almost negligible and the oxidation reaction was carried out at 140 ºC, achieving a conversion of

about 20 % at 32 h. This relative reactivity order can be easily explained assuming that the reaction takes place inside the pores of MIL-101-(Cr)-NO_2 particles and considering the relative diffusion coefficient as the molecular dimensions of the substrates increases. [17, 21] Therefore, the larger the substrate, the slower should be the reaction due to the impeded diffusion of the substrate inside the MOF crystal.

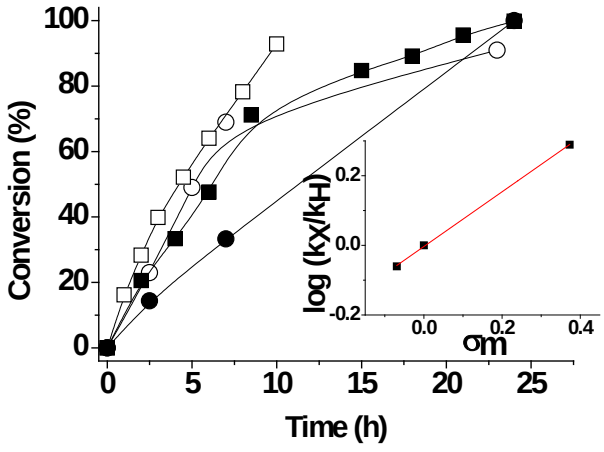

Figure 16. Time-conversion plot for the aerobic oxidation of benzylamine (■), 4-chlorobenzylamine (□), 2-picolylamine (○), 4-methylbenzylamine (●) to the corresponding substituted N-benzylidene benzylamines using MIL-101(Cr)-NO_2 as catalyst. Plot of the relative initial reaction rate in logarithmic scale versus the σ_m Hammett constant. Reaction conditions: Catalyst (12 mg, 0.04mmol of Cr), substrate (20 mmol), O_2 atmosphere.

3. Conclusions

Going beyond the state of the art that has shown the influence of the presence of substituents in UiO-66 for Lewis acid catalyzed reactions, in the present work we have shown that also for aerobic oxidations the nature of the substituent on the linker plays a key role on the activity of a different MOF as promoter. This finding is particularly remarkable since the available mechanistic data indicate that the role of MIL-101 for this reaction type is not really catalytic, but more as a promoter generating ROS from molecular oxygen. Electrochemical data have shown that the presence of the substituent on the terephthalate linker modifies the redox potential of the Cr^{3+} ions in the nodes and this is beneficial for the promotion of aerobic oxidation when electron withdrawing groups are present on the terephthalate linkers. It has been demonstrated that MIL-101(Cr)-NO_2 does not deactivate under the reaction conditions and, that it has a wide scope of benzylamine substrates, whose reactivity increases with the presence of electron withdrawing substituents on the aromatic ring. From the relative reactivity order that is basically controlled by molecular size it is proposed that the reaction takes place predominantly in the interior of the MOFs crystallites. Overall the present data shows the flexibility that MOFs offer for improvement of the catalytic performance by introducing proper substituents on the organic linker that modulate the electron density around metal nodes acting as active sites.

4. Experimental Section

4.1. Materials

All the reagents and solvents used in this work were of analytical or HPLC grade and supplied by Sigma-Aldrich. Benzylamines were freshly distilled before use.

4.2. Catalyst preparation

MIL-101(Cr)-H and their isoestructural MIL-101(Cr)-X derivatives have been synthesized according reported procedures. [10, 34] Briefly, the corresponding terephthalic acid derivative (1.5 mmol) and $Cr(NO_3)_3{\cdot}9H_2O$ or $CrCl_3$ (for the synthesis of MIL-101(Cr)-X (X: NO_2, Cl, CH_3) (1 mmol) were added to a Teflon autoclave containing 8 mL of demineralized water. Then, in the case of MIL-101(Cr)-H 10 µL of HF were added. The autoclave was heated at the corresponding temperature for a determined period of time (Table 4). After cooling to room temperature, the resulting precipitate was washed several times with DMF and ethanol at 120 and 80 ºC, respectively. In the case of MIL-101(Cr)-SO_3H the material was obtained by post-synthetic sulfonation of preformed MIL-101(Cr)-H with chlorosulfonic acid, as reported in the literature.[44] The MIL-101(Cr)-NH_2 material was obtained by post-synthetic reduction of preformed MIL-101(Cr)-NO_2 with $SnCl_2{\cdot}H_2O$ following reported procedures.[45]

Table 4. Autoclave preparation conditions of the MIL-101(Cr) materials used in this work.

	Temperature (ºC)	Time (h)
MIL-101(Cr)-H	200	8
MIL-101(Cr)-NO_2	180	120
MIL-101(Cr)-Cl	180	96
MIL-101(Cr)-CH_3	180	120

4.3. Catalyst characterization

X-ray diffractograms of MIL-101(Cr) were recorded using a Philips XPert diffractometer equipped with a graphite monochromator (40 kV and 45 mA) employing Ni filtered CuKα radiation. The N2 adsorption isotherms at 77 K were measured using an ASAP 2010 Micrometrics device. ATR-FTIR spectra of room temperature equilibrated MIL-101(Cr)-X samples were recorded by using a Bruker Tensor27 instrument. Prior the measurements the samples were heated in an oven at

100 ºC for 12 h to remove physisorbed water. Termogravimetry measurements were performed using a TGA/SDTA851e and a TSO801RO METTLE TOLEDO. Cyclic voltammograms of the prepared MIL-101(Cr)-X (X: H, NO_2, Cl, SO_3H) materials were obtained by using a Princeton Applied Research VersaSTAT 3.

4.4. Catalytic experiments

Typically, the required amount of MIL-101(Cr)-X (X: H, NO_2, NH_2, Cl, CH_3) catalyst (0.04 mmol of Cr with respect to benzylamine) was added to a double-neck round-bottom flask (25 mL). To generate coordinatively unsaturated sites in the metal clusters of MIL-101(Cr)-X materials were pretreated by heating them at 150 ºC under vacuum overnight. The required amount of substrate (i.e. 20 mmol) was introduced into the flask and the system sonicated for 20 min. Subsequently, the reaction mixture was placed in a bath preheated at the required reaction temperature (i.e. 120 ºC) and magnetically stirred.

Selective radical quenching experiments were carried out following the general procedure, but with the addition of radical quenchers (20 mol % respect to substrate) including dimethylsulfoxide (DMSO), p-benzoquinone or 2,2,6,6-tetramethyl-1-piperidinyloxy (TEMPO) at about 35 % conversion.

Reuse experiments for the most active MIL-101(Cr)-NO_2 sample were performed under the general reaction conditions. At the end of each reaction, the solid catalyst was filtered through a Nylon membrane filter (0.2 µm), placed in a round-bottom flask containing ethanol and heated at 80 ºC for 2 h. This procedure was repeated two more times. Then, the catalyst was dried at 100 ºC for 24 h. The catalyst was thermally activated at 150 ºC under vacuum and used as indicated before.

4.5. EPR measurements

MIL-101(Cr)-H or MIL-101(Cr)-NO_2 (5 mg) was added to a round bottom flask (25 mL) containing N-tert-butyl-α-phenylnitrone (PBN, 1150 mg L-1) dissolved in n-dodecane (10 mL). Then, the flask was sonicated (20 min) and purged with a balloon containing O_2. Finally, the system was heated at 120 °C for 4 h. Then, an aliquot was filtered (Nylon filter, 0.2 µm) and the sample purged with N_2 before recording the EPR. EPR spectra were acquired using a Bruker EMX instrument with the following parameters: frequency 9.803 GHz, sweep width 3489.9 G, time constant 40.95 ms, modulation frequency 100 kHz, modulation width 1 G, microwave power 19.92 mW.

4.6. Product analysis

Previously filtered reaction aliquots were diluted in a toluene solution containing a known amount of nitrobenzene as external standard. Subsequently, the aliquots were analyzed by gas chromatography using a flame ionization detector. Quantification was carried out by using calibration curves of authentic samples.

4.7. H_2O_2 measurements

Previously filtered reaction aliquots (0.5 mL) were put in contact with distilled water (4.5 mL). After phase separation, a titanium oxalate solution ($K_2(TiO)(C_2O_4)_2$ in H_2SO_4/HNO_3; 0.5 mL)) was added as a colorimetric titrating agent and allowed to react for 10 min. The intensity of the developed yellow color was monitored at λ=420 nm.

4.8. Leaching experiments

At the end of the reaction, the catalyst was removed by filtration. Then, the organic phase was stirred with an HNO_3 aqueous solution (3 M), and the system heated at 80 ºC for 24 h to extract Cr^{3+} ions. The presence of chromium in the aqueous phase was analyzed by chemical analysis using an ICP-AES instrument.

Acknowledgements

Financial support by the Spanish Ministry of Economy and Competitiveness (CTQ 2015-69153-CO2-1, CTQ2014-53292-R, Severo Ochoa) and Generalitat Valenciana (Prometeo 2013-014) is gratefully acknowledged.

Notes and references

1. A. Corma, H. Garcia and F. X. Llabrés i Xamena, *Chem. Rev.*, 2010, **110**, 4606-4655.
2. A. Dhakshinamoorthy, Opanasenko, M., Čejka, J., Garcia, H., *Catal. Sci. Technol.*, 2013, **3**, 2509-2540.
3. A. Dhakshinamoorthy, M. Alvaro and H. Garcia, *Catal. Sci. Technol.*, 2011, **1**, 856-867.
4. J. Gascon, A. Corma, F. Kapteijn and F. X. Llabrés i Xamena, *ACS Catal.*, 2014, **4**, 361-378.
5. M. Yoon, R. Srirambalaji and K. Kim, *Chem. Rev.*, 2012, **112**, 1196-1231.
6. H. Furukawa, Cordova, K.E., O'Keeffe, M., Yaghi, O.M., *Science*, 2013, **341**, 1230444.
7. A. H. Chughtai, N. Ahmad, H. A. Younus, A. Laypkov and F. Verpoort, *Chem. Soc. Rev.*, 2015, **44**, 6804-6849.
8. O. A. Kholdeeva, *Catal. Today*, 2016, **278**, 22-29.

9. T. Devic and C. Serre, *Chem.Soc.Rev.*,, 2014, **43**, 6097-6115.
10. G. Ferey, C. Mellot-Draznieks, C. Serre, F. Millange, J. Dutour, S. Surble and I. Margiolaki, *Science*, 2005, **309**, 2040-2042.
11. S. Kitagawa, R. Kitaura and S.-I. Noro, *Angew. Chem., Int. Ed.*, 2004, **43**, 2334-2237.
12. Y. F. Chen, R. Babarao, S. I. Sandler and J. W. Jiang, *Langmuir*, 2010, **26**, 8743-8750.
13. S. H. Jhung, J.-H. Lee, J. W. Yoon, C. Serre, G. Férey and J.-S. Chang, *Adv. Mater.* , 121-124.
14. N. V. Maksimchuk, O. V. Zalomaeva, I. Y. Skobelev, K. A. Kovalenko, V. P. Fedin and O. A. Kholdeeva, *Proc. R. Soc. A*, 2012, **468**, 2017-2034.
15. A. Demessence, P. Patricia Horcajada, C. Christian Serre, C. C. Boissière, D. Grosso, C. Sanchez and G. Férey, *Chem. Commun.*, 2009, 7149-7151.
16. N. V. Maksimchuk, K. A. Kovalenko, V. P. Fedin and O. A. Kholdeeva, *Chem. Comm.*, 2012, **48**, 6812-6814.
17. A. Santiago-Portillo, S. Navalon, F. Cirujano, F. Llabrés i Xamena, M. Alvaro and H. Garcia, *ACS Catal.*, 2015, **5**, 3216–3224.
18. O. A. Kholdeeva, I. Y. Skobelev, I. D. Ivanchikova, K. A. Kovalenko, V. P. Fedin and A. B. Sorokin, *Catal. Today*, 2014, **238**, 54-61.
19. I. Y. Skobelev, K. A. Kovalenko, V. P. Fedin, A. B. Sorokin and O. A. Kholdeeva, *Kinet. Catal.*, 2013, **54**, 607-614.
20. I. Y. Skobelev, A. B. Sorokin, K. A. Kovalenko, V. P. Fedin and O. A. Kholdeeva, *J. Catal.*, 2013, **298**, 61-69.
21. A. Gómez-Paricio, A. Santiago-Portillo, S. Navalón, P. Concepción, M. Alvaro and H. Garcia, *Green Chem.*, 2016, 508-515.
22. R. Guo, J. Bai, H. Zhang, Y. Xie and J. Li, *Prog. Chem.*, 2016, **28**, 232-243.
23. A. Dhakshinamoorthy, A. M. Asiri and H. Garcia, *Chem. Eur. J.*, 2016, **22**, 8012-8024.
24. F. X. Llabrés i Xamena, O. Casanova, R. Galiasso Tailleur, H. Garcia and A. Corma, *J. Catal.*, 2008, **255**, 220-227.
25. I. Luz, A. León, M. Boronat, F. X. Llabrés i Xamena and A. Corma, *Catal. Sci. Technol.*, 2013, **3**, 371-379.
26. A. Dhakshinamoorthy, M. Alvaro and H. Garcia, *ChemCatChem*, 2010, **2**, 1438-1443.
27. A. Dhakshinamoorthy, M. Alvaro, P. Horcajada, E. Gibson, M. Vishnuvarthan, A. Vimont, J.-M. Grenèche, C. Serre, M. Daturi and H. Garcia, *ACS Catal.*, 2012, **2**, 2060-2065.
28. F. Vermoortele, M. Vandichel, B. V. de Voorde, R. Ameloot, M. Waroquier, V. Van Speybroeck and D. E. De Vos, *Angew. Chem. Int. Ed.*, 2012, **51**, 4887-4890.
29. S. M. Cohen, *Chem. Rev.*, 2012, **112**, 970-1000.
30. K. K. Tanabe and S. M. Cohen, *Chem. Soc. Rev.*, 2011, **40**, 498-519.
31. M. Ranocchiari, Bokhoven, J.A.V., *Phys. Chem. Chem. Phys.*, 2011, **13**, 6388-6396.
32. C. Wang, Zheng, M., Lin, W., *J. Phys. Chem. Lett.*, 2011, **2**, 1701-1709.
33. J. Liu, L. Chen, H. Cui, J. Zhang, L. Zhang and C.-Y. Su, *Chem. Soc. Rev.*, 2014, **43**, 6011-6061.
34. M. Lammert, S. Bernt, F. Vermoortele, D. E. De Vos and N. Stock, *Inorg. Chem.*, 2013, **52**, 8521–8528.
35. M. Saikia and L. Saikia, *RSC Adv.*, 2016, **6**, 15846-15853.
36. Y. Luan, Y. Qi, H. Gao, R. S. Andriamitantsoa, N. Zheng and G. Wang, *J. Mater. Chem. A*, 2015, **3**, 17320-17331.
37. B. Li, K. Leng, Y. Zhang, J. J. Dynes, J. Wang, Y. Hu, D. Ma, Z. Shi, L. Zhu, D. Zhang, Y. Sun, M. Chrzanowski and S. Ma, *J. Am. Chem. Soc.*, 2015, **137**, 4243-4248.
38. D. Wang and Z. Li, *Catal. Sci. Technol.*, 2015, **5**, 1623-1628.
39. Y. X. Zhou, Y. Z. Chen, Y. Hu, G. Huang, S. H. Yu and H. L. Jiang, *Chem. Eur. J.*, 2014, **20**, 14976-14980.
40. Z. Hasan, J. W. Jun and S. H. Jhung, *Chem. Eng. J.*, 2015, **278**, 265-271.
41. Y. Jin, J. Shi, F. Zhang, Y. Zhong and W. Zhu, *J. Mol. Catal. A.-Chem.*, 2014, **383-384**, 167-171.
42. Y. Zang, J. Shi, F. Zhang, Y. Zhong and W. Zhu, *Catal. Sci. Technol.*, 2013, **3**, 2044-2049.
43. M. Hartmann and M. Fischer, *Micropor. Mesopor. Mater.*, 2012, **164**, 38-43.
44. B. Li, Y. Zhang, D. Ma, L. Li, G. Li, G. Li, Z. Shi and S. Feng, *Chem. Commun.*, 2012, **48**, 6151-6153.
45. S. Bernt, V. Guillerm, C. Serre and N. Stock, *Chem. Commun.*, 2011, **47**, 2838-2840.
46. A. Grirrane, A. Corma and H. Garcia, *J. Catal.*, 2009, 138-144.
47. S. Navalon, A. Dhakshinamoorthy, M. Alvaro and H. Garcia, *Chemical Reviews*, **114**, 6179-6212.
48. C. Su, M. Acik, K. Takai, J. Lu, S.-J. Hao, Y. Zheng, P. Wu, Q. Bao, T. Enoki, Y. J. Chabal and K. P. Loh, *Nat. Commun.*, 2012, **3**, 2315.
49. P. Valvekens, F. Vermoortele and D. De Vos, *Catal. Sci. Technol.*, 2013, **3**, 1435-1445.
50. N. A. Milas, *Chem. Rev.*, 1932, **10**, 295-364.
51. E. G. Janzen, Y. Kotake and H. Randall D., *Free Radical Bio. Med.*, 1992, **12**, 169-173.
52. E. G. Janzen, R. D. Hinton and Y. Kotake, *Tetrahedron Lett.*, 1992, **33**, 1257-1260.
53. M. J. Burkitt and R. P. Mason, *Proc. Natl. Acad. Sci. USA*, 1991, **88**, 8440-8444.
54. R. Martin, S. Navalon, J. J. Delgado, J. J. Calvino, M. Alvaro and H. Garcia, *Chem. - Eur. J.* , 2011, **17**, 9494–9502.
55. A. Dhakshinamoorthy, S. Navalon, M. Alvaro and H. Garcia, *ChemSusChem*, 2012, **5**, 46-64.
56. Y. Wang, Y. Xie, H. Sun, J. Xiao, H. Cao and S. Wang, *ACS Appl. Mater. Interfaces*, 2016, **8**, 9710–9720.

